Biol. Chem., Vol. 388, pp. 523–531, May 2007 • Copyright © by Walter de Gruyter • Berlin • New York. DOI 10.1515/BC.2007.060

Two α subunits and one β subunit of meprin zinc-endopeptidases are differentially expressed in the zebrafish *Danio rerio*

Andre Schütte[1], Daniel Lottaz[2], Erwin E. Sterchi[2], Walter Stöcker[1] and Christoph Becker-Pauly[1,*]

[1] Institute of Zoology, Johannes Gutenberg-University, Johannes-von-Müller-Weg 6, D-55128 Mainz, Germany
[2] Institute of Biochemistry and Molecular Medicine, University of Bern, Bühlstraße 28, CH-3012 Bern, Switzerland

* Corresponding author
e-mail: beckerpa@uni-mainz.de

Abstract

Meprins are members of the astacin family of metalloproteases expressed in epithelial tissues, intestinal leukocytes and certain cancer cells. In mammals, there are two homologous subunits, which form complex glycosylated disulfide-bonded homo- and heterooligomers. Both human meprin α and meprin β cleave several basement membrane components, suggesting a role in epithelial differentiation and cell migration. There is also evidence that meprin β is involved in immune defence owing to its capability of activating interleukin-1β and the diminished mobility of intestinal leukocytes in meprin β-knockout mice. Here we show for the first time by reverse transcription PCR, immunoblotting and immunofluorescence analyses that meprins are expressed not only in mammals, but also in the zebrafish *Danio rerio*. In contrast to the human, mouse and rat enzymes, zebrafish meprins are encoded by three genes, corresponding to two homologous α subunits and one β subunit. Observations at both the mRNA and protein level indicate a broad distribution of meprins in zebrafish. However, there are strikingly different expression patterns of the three subunits, which is consistent with meprin expression in mammals. Hence, *D. rerio* appears to be a suitable model to gain insight into the basic physiological functions of meprin metalloproteases.

Keywords: astacin; metalloprotease; metzincin; zebrafish.

Introduction

Meprins are members of the astacin family of endopeptidases (Bond and Beynon, 1995). They contain the conserved zinc-binding motif (HExxHxxGxxHxxxRxDR) and a methionine-containing 1,4-β-turn (SxMHY) typical for the metzincins (Stöcker et al., 1993, 1995; Gomis-Rüth, 2003). Mammalian meprins comprise two homologous, highly glycosylated multidomain subunits, α and β, of approximately 75 and 85 kDa, respectively (Becker et al., 2003; Bertenshaw et al., 2003). The two subunits are encoded on chromosomes 6 and 18 in humans and 17 and 18 in mice, respectively (Bond et al., 1995). Meprins are translated with an amino-terminal signal peptide directing the protein chain to the endoplasmic reticulum, an amino-terminal propeptide, an astacin-like protease domain, a MAM (meprin A5 protein tyrosine phosphatase μ) and a TRAF domain (tumour necrosis factor receptor-associated factor), which are thought to mediate protein-protein interactions, followed by an EGF (epidermal growth factor)-like module, the C-terminal transmembrane domain and a cytosolic tail (Ishmael et al., 2005). In contrast to the β subunit, meprin α contains an additional inserted domain (I-domain) that is proteolytically cleaved on the secretory pathway, resulting in the loss of the EGF-like and the transmembrane domains and secretion into the extracellular space. While meprin β is integrated into the plasma membrane as a type I integral protein, in human cells it may also be shed from there (Johnson and Hersh, 1994; Hahn et al., 2003). If expressed alone, both meprin subunits form homooligomers. These can reach a size of several megadaltons in the case of meprin α, whereas the β subunits merely form homodimers. If α and β are coexpressed, they are organised as heterodimers and (mostly) heterotetramers (Bertenshaw et al., 2003).

Proteases of the astacin family are synthesised as zymogens, and thus need to be activated by cleavage of the propeptide to gain full proteolytic activity (Yiallouros et al., 2002). In the case of meprins, this activation is mostly achieved by serine proteases such as trypsin, whereas many other astacins, such as BMP-1, are activated by the proprotein convertase furin (Bode et al., 1992; Leighton and Kadler, 2003). Outside the intestinal tract, in the absence of pancreatic trypsin, promeprin α, but not β, can be activated by plasmin, as shown in colorectal cancer cells (Rösmann et al., 2002; Becker et al., 2003). Recently we demonstrated that promeprin β, but not α can be activated by human kallikrein-4 in human skin (Becker-Pauly et al., 2007).

Both meprin subunits cleave a wide range of proteins and biologically active peptides, although they differ considerably in their cleavage specificity (Kruse et al., 2004). They can process compounds of the extracellular matrix such as laminin-V, collagen-IV, fibronectin and nidogen 1, as well as growth factors, cytokines and peptide hormones, including bradykinin, angiotensins and gastrin (Yamaguchi et al., 1992; Skidgel, 1992; Bertenshaw et al., 2001; Kruse et al., 2004). Furthermore, the ability of meprin β to activate interleukin-1β is indicative of a role for meprins in the immune system (Herzog et al., 2005). These observations are supported by the work of Cris-

man et al. (2004), who showed that compared to leukocytes from wild-type animals, macrophages from meprin β knockout mice exhibited retarded migration through the extracellular matrix, resulting in a diminished immune response (Crisman et al., 2004). In general, meprin β knockout mice are viable and do not show a dramatic phenotype, but their offspring are smaller than wild-type littermates and the newborn grow more slowly (Norman et al., 2003).

Meprin zinc-endopeptidases were originally found in the epithelia of proximal tubules of mouse kidney and in brush border membranes of human intestine (Sterchi et al., 1982, 1983, 1988). Other meprin-expressing tissues such as spleen, pancreas and liver were identified via EST analyses (Merops peptidase database, http://merops.sanger.ac.uk; EMBL-EBI ArrayExpress Warehouse, http://www.ebi.ac.uk/aedw). The enzyme was also found in human skin epithelia, in leukocytes of the intestinal lamina propria mucosae and in colorectal cancer cells (Lottaz et al., 1999a,b; Becker-Pauly et al., 2007). In these cultured colon carcinoma cells, meprin α is secreted not only apically, but also basolaterally. Hence, the proteolytic potential of meprins is directed towards the extracellular matrix, which may effect the proliferation and migration of tumour cells into the surrounding tissue (Kaushal et al., 1994). Similar observations have been made in mice suffering from acute renal failure (Kaushal et al., 1994; Trachtman et al., 1995). Carmago et al. (2002) demonstrated that a mixture of meprin α homooligomers and α/β heterooligomers has a negative effect on the viability of certain strains of kidney cells (LLC-PK_1, immortalised porcine epithelial cells and MDCK, Madin-Darby canine kidney cells). Furthermore, it was shown that meprin β can reduce the cell number of cultured keratinocytes (HaCaT) by inducing apoptosis (Becker-Pauly et al., 2007).

Taken together, these findings suggest a contribution of meprins to epithelial differentiation, matrix remodelling and cell migration, as well as to inflammatory processes, tumour growth and metastasis. *In vivo* substrates of meprins are known, but precise biological mechanisms have not been elucidated yet. In this context we suggest that the zebrafish *Danio rerio* might be a suitable model to gain insight into the physiological functions of meprins (Trede et al., 2004).

In the present work we identified three individual meprin subunits in *Danio rerio*. They are expressed in kidney, liver, intestine, epidermis, brain, heart and gills, albeit at different levels. Varying residues around the active site cleft that are critical for cleavage specificity support this individuality. The domain structure of the meprins described reveals striking differences compared to mammalian homologues. For example, one α subunit lacks the C-terminus including the I-domain, most probably resulting in a soluble form without posttranslational processing. In the case of meprin β, no EGF-like domain could be identified so far. These differences in expression and domain structure indicate unique functions for each subunit.

Results

Three individual subunits of zebrafish meprin are encoded on chromosome 20

Database analyses of the *Danio rerio* genome revealed three genes encoding meprin α subunits [Swiss-Prot accession nos. Q5RHM1, Q5RKM1 (both meprin α_1) and Q5RHM2 (meprin α_2)]. The first and second one turned out to be identical, probably due to gene duplication. In contrast, a single gene encodes the meprin β subunit, as observed for other classes of vertebrates (Swiss-Prot accession no. Q5RH57). All genes are localised on chromosome 20 (α_1 from 26 340 765 to 26 349 044 bp and α_2 from 26 352 145 to 26 363 302 bp), whereas the β gene is located further upstream (from 44 259 211 to 44 276 969 bp; Vertebrate Genome Annotations database, http://vega.sanger.ac.uk). As the meprin α_1 cDNA deposited in the database was only a fragment, we identified the 3′-end including the amino-terminal signal peptide by *in silico* analyses of genomic DNA. Interestingly, zebrafish meprin α_1 cDNA contains a stop codon immediately downstream of the region encoding the TRAF domain. Therefore, zebrafish meprin α_1 does not contain EGF-like, transmembrane or cytosolic domains (Figure 1). Furthermore, the typical RxK(or R)R sequence in the

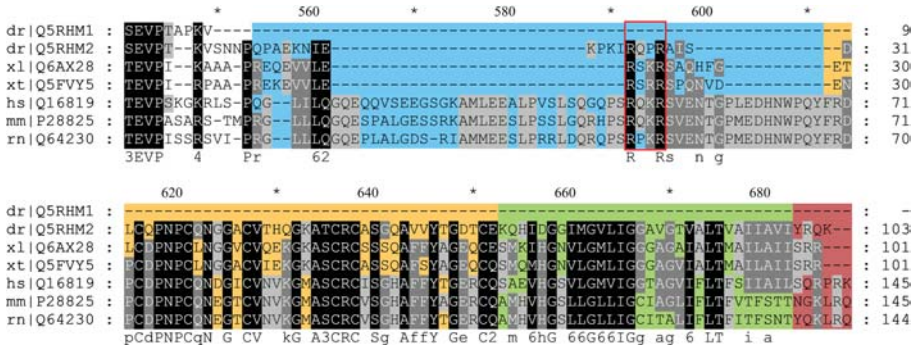

Figure 1 Alignment of the C-terminal domains of meprin α subunits.
In contrast to other vertebrate meprins, the zebrafish α_1 subunit has a truncated domain structure. The inserted domain, which is fragmented in zebrafish α_2 and *Xenopus* meprins, is highlighted in blue. Putative furin-like recognition sequences are marked by a red box. The EGF domain, containing six cysteine residues, is indicated in orange and the transmembrane domain in green. The cytosolic tail is displayed in dark red. Species names and Swiss-Prot accession numbers are shown in the left column (dr, *Danio rerio*; xl, *Xenopus laevis*; xt, *Xenopus tropicalis*; hs, *Homo sapiens*; mm, *Mus musculus*; rn, *Rattus norvegicus*).

I-domain, which is present in all mammalian and in amphibian (*Xenopus)* meprin α chains, is a potential cleavage site for the prohormone convertase furin. This motif is mutated in meprin α_2 of *Danio rerio* to RxPR, which might influence proteolytic processing during biosynthesis.

Sequence alignment of the catalytic domains demonstrates the high similarity to other astacins, particularly to mammalian meprins (Figure 2). The meprin α_1 and α_2 subunits of zebrafish show 71% identity to each other and 68% and 71% to human α, respectively. The two α subunits are 54% and 57% identical to zebrafish β. In all aligned sequences, the typical zinc-binding motif and the methionine turn are present. However, there is a significant point mutation in the HExxHxxGxxHE sequence of zebrafish meprin α_1, whereby the second glutamate (Glu101) found in all other meprins and most astacins is mutated to a methionine (Met101) (Figure 2). Based on this alignment, a phylogenetic tree was computed to visualise the evolutionary correlation between meprins from different organisms on a molecular level (Figure 3). All proteases exhibit subunit-specific clustering, with the β cluster branching before α. This provides evidence that the β subunit is the phylogenetic precursor of other meprin subunits. Moreover, all zebrafish meprins separate early from their mammalian homologues. Meprin α_1 with the mutated zinc-binding motif branches most basically and seems to be more distantly related to mammalian meprin α than the α_2 subunit of *D. rerio.*

In comparison to other meprins, zebrafish homologues show significant differences in residues critical for cleavage specificity

Based on the crystal structure of crayfish astacin, three-dimensional homology models of the catalytic domains of zebrafish and human meprins were generated (Figure 4). The zinc-binding motif, the Met-turn and the astacin-typical secondary structure elements, comprising a five stranded β-sheet and four α-helices, are displayed in a ribbon model in Figure 4A–C. The surface models visualise significant differences with regard to basic and acidic residues in the substrate-binding region (Figure 4D–H). Human meprin β has positively charged Arg85 and Arg123 (Figure 4H), which might be responsible for the distinct substrate specificity for negatively charged side chains of this subunit (Bertenshaw et al., 2001). In zebrafish meprin β, only Lys123 was identified as a positively charged residue around the active site (Figure 4F). Zebrafish meprin α_1 contains Asp61, which is also in human meprin α (Figure 4G), and Arg150 (Figure 4D). The α_2 subunit has other charged residues on the outskirts of the active site region, namely Glu80 and a Lys122 (Figure 4E).

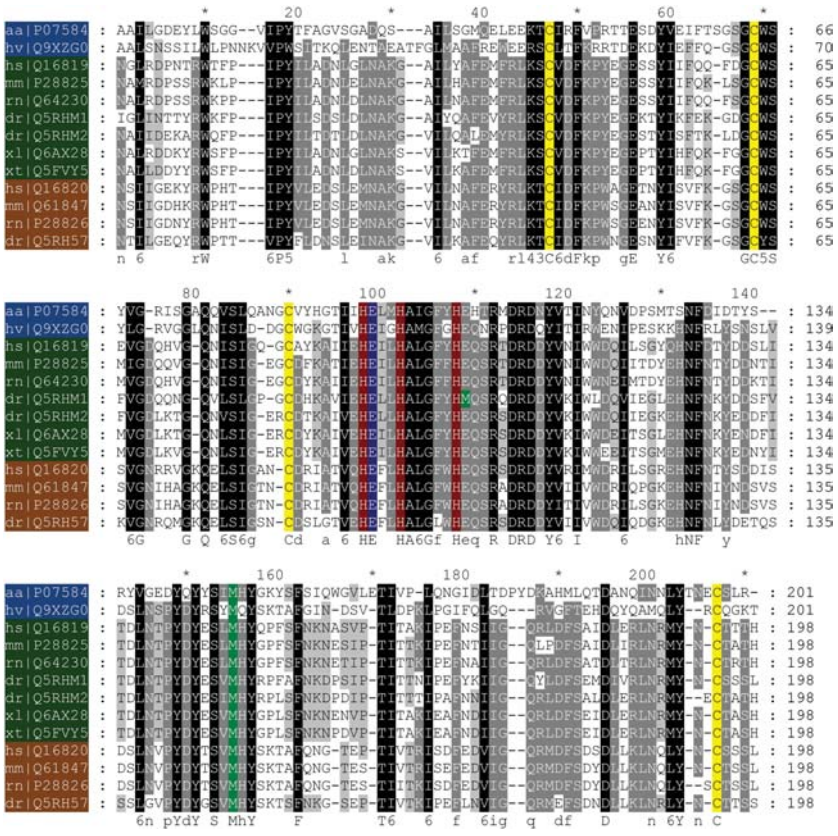

Figure 2 Alignment of the amino acid sequences of the catalytic domains of vertebrate meprins and astacins of crayfish and hydra. The labels provide the species names and the Swiss-Prot accession numbers (aa, *Astacus astacus*; hv, *Hydra vulgaris*; hs, *Homo sapiens*; mm, *Mus musculus*; rn, *Rattus norvegicus*; dr, *Danio rerio*; xl, *Xenopus laevis*; xt, *Xenopus tropicalis*). Astacins are shown in blue, meprin α subunits in green, and meprin β subunits in brown. The three histidines belonging to the characteristic zinc-binding motif are highlighted in red. The catalytic active glutamate is marked in blue. In all sequences, four cysteines (yellow) forming two disulfide bonds are evident. Methionines in the zinc-binding motif of meprin α_1 and in the typical met-turn of all astacins displayed are coloured in green.

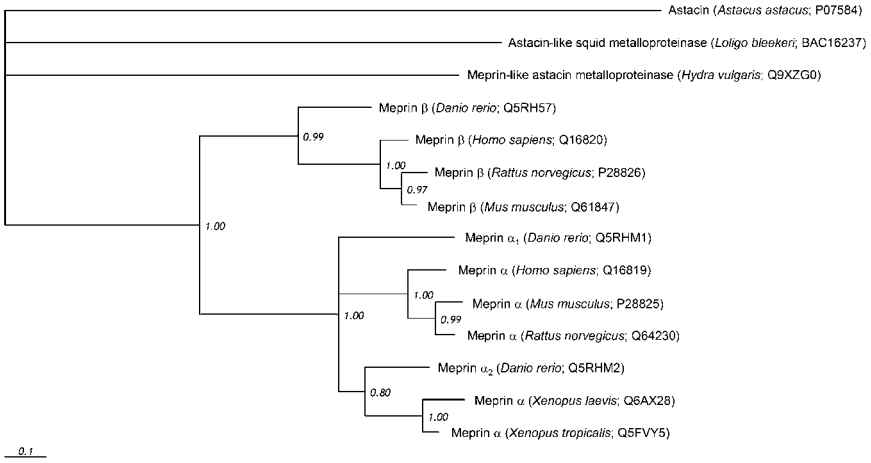

Figure 3 Phylogenetic tree of meprins and astacins from different species.
The numbers show the relative probability of branching (1.00 corresponds to 100%). Astacin from crayfish *Astacus astacus* was defined as an outgroup.

mRNA of the meprin subunits is expressed in different zebrafish tissues

The three meprin subunits could be identified in different zebrafish tissues by RT-PCR. After isolation of the RNA and reverse transcription into cDNA, PCR was performed with primers specific for each meprin subunit gene. These primers flank cDNA fragments of 381 bp for meprin α_1, 405 bp for meprin α_2 and 442 bp for meprin β. Except for meprin α_1, which was absent from kidney, all other subunits were detected in kidney, intestine, liver, gills, brain, heart and epidermis, albeit at different intensities (Figure 5A).

Meprins are detected in zebrafish lysates by Western blot analysis

For the detection of zebrafish meprins, polyclonal antisera directed against human meprin subunits were applied. Two antibodies generated against peptides spanning the catalytic domains of human meprin α and β were found to cross-react with zebrafish meprins because of the high sequence similarity of the protease domains of human and fish enzymes. To demonstrate meprin expression by Western blotting, total zebrafish lysates of three individual animals were analysed (Figure 5B). In all samples, a single band could be identified corresponding to a molecular mass of about 73 kDa (Figure 5B, lanes 2–5). Compared to the recombinant proforms of human meprins from insect cells with a molecular mass of approximately 78 kDa (Figure 5B, lanes 6 and 7) it is most likely that the visualised bands in the lysate samples correspond to active meprin α_1 and α_2. However, it is not clear whether zebrafish meprins are as highly glycosylated as mammalian meprins.

Distribution of meprins in zebrafish visualised by immunofluorescence microscopy

The antisera directed against human meprins were also used to analyse cryosections of zebrafish whole mounts for meprin expression (Figure 6). The fluorescence signals obtained by the antisera were localised to head kidney, epidermis, gills and intestine. These sites of meprin expression confirm in part the reported expression sites in mammals, as well as the results obtained by RT-PCR for zebrafish tissues (Figure 5A).

Table 1 provides a summary of all identified zebrafish tissues expressing meprins in comparison to their mammalian homologues. It is evident that meprin expression is not restricted to certain tissues, but is widely distributed over a variety of vertebrate epithelia.

Discussion

So far, meprins were only reported to exist in mammals (human, mouse and rat). Based on genomic sequences, meprin homologues could also be found in several other vertebrate taxa, e.g., in the clawed frog *Xenopus laevis* [Swiss-Prot accession no. Q6AX28] and *Xenopus tropicalis* [Swiss-Prot accession no. Q5FVY5]. Here we have reported on four cDNA sequences encoding three meprin subunits in the zebrafish *D. rerio.* We identified the critical amino acid residues in the active site, which presumably define substrate specificity, and revealed their expression and tissue distribution at the mRNA and protein levels in zebrafish.

In contrast to mammalian meprins, three meprin genes were found in zebrafish by database analyses. They encode two different α subunits [Swiss-Prot accession nos. Q5RHM1 (meprin α_1) and Q5RHM2 (meprin α_2)] and one β subunit [Swiss-Prot accession no. Q5RH57]. In humans, the gene encoding meprin α is located on chromosome 6 close to the gene of the major histocompatibility complex II (MHC II), whereas the gene for meprin β is on chromosome 18. In the mouse genome, the latter gene is also on chromosome 18, while the gene for meprin α is encoded on chromosome 17. Both subunits are expressed coordinately and separately in mammals. In contrast to the genomic localisation of meprin genes in mammals, all three zebrafish meprin genes are encoded on chromosome 20. The two genes coding for the α subunit are in close proximity. The co-transcriptional processes observed in mammals are also conceivable in

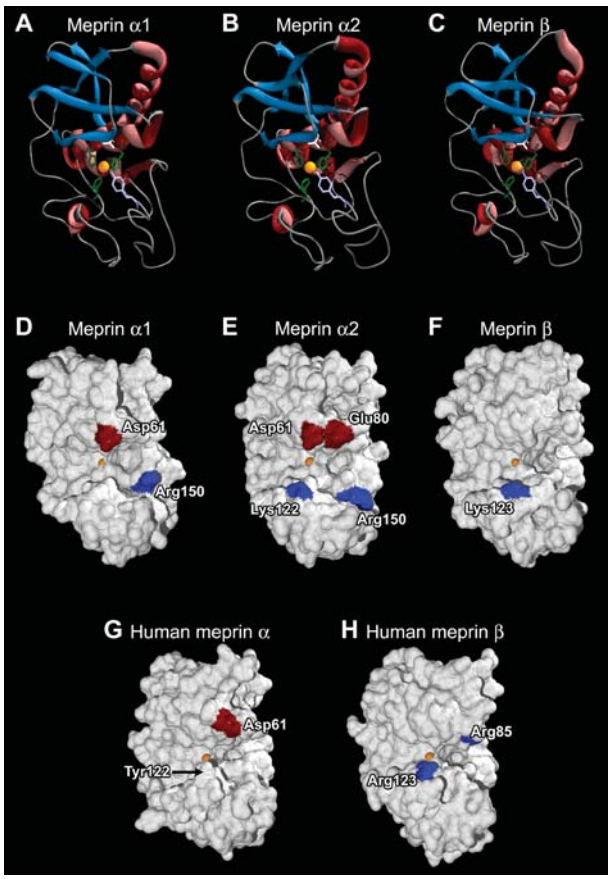

Figure 4 Homology models of the catalytic domains of zebrafish and human meprins.
The ribbon models (A–C) show the active site with the zinc ion in its centre (orange), complexed by three histidines (green). The catalytically active glutamate (white) and the fifth zinc ligand tyrosine (lilac) rise into the active site cleft. Astacin characteristic secondary structural elements are marked in blue (β-strands) and red (α-helices). The homology surface models (D–H) were computed based on the crystal structure of astacin from *Astacus astacus*. All zebrafish subunits (D–F) differ in characteristic acidic (red) and basic (blue) residues around the cleavage site with the central zinc ion (orange). In zebrafish, meprin α_1 offers Asp61 and Arg150 (D), while meprin α_2 additionally offers Glu80 and Lys122 (E). The meprin β subunit possesses only one basic residue (Lys123) around the active site (F). Critical residues in human meprins are Asp61 and Tyr122 (arrow) in the α subunit (G), and Arg85 and Arg123 in the β subunit (H).

zebrafish. The existence of two different α subunits and their local proximity at the chromosomal level could be due to single gene duplication. Interestingly, the sequences of the two α subunits have diverged considerably, resulting in an overall sequence identity of approximately 48%. Both α subunits are expressed at the mRNA level, and hence they are both presumably translated, but the functional properties of the proteins remain to be proven.

All three meprin subunits identified in zebrafish contain the typical astacin domain. The zinc-binding motif [HExxHxxGxxHE(or M)], the Met-turn (SxMHY) and the four cysteine residues that form two disulfide bonds are highly conserved in all mammalian, amphibian and fish meprins. Interestingly, in the α_1 subunit of *D. rerio*, the second glutamate (Glu101) of the zinc-binding motif is mutated to a methionine. In astacin, the corresponding glutamate (Glu103) is responsible for a salt bridge to the mature N-terminus (Stöcker et al., 1993). By mutating this glutamate to an alanine in crayfish astacin, Stöcker and co-workers showed that the enzyme is more active than the wild-type protease, but is extremely heat labile (Yiallouros et al., 2002). Therefore, zebrafish meprin α_1 could be as active, but not as stable as the mammalian subunit. This may be a regulatory mechanism to diminish extended meprin activity by easier degradation of the protein. The mutation of this second glutamate in the zinc-binding motif could also be rarely observed in other astacins, although this has never been analysed at the protein functional level.

Zebrafish meprin α subunits also differ from mammalian meprins regarding their C-terminal domains. It is apparent that meprin α_1 and α_2 do not contain a complete I-domain. Interestingly, this is the same for *Xenopus* meprins, indicating that a complete I-domain might be specific for mammals. Furthermore, the furin cleavage site RxK(or R)R, which might be responsible for proteolytic processing of meprin α during biosynthesis, resulting in a secreted homooligomer, is mutated to RxPR in the α_2 subunit. Furin-like proteases are able to cleave RxxR sites, albeit with lower cleavage efficiency (Duckert et al., 2004; Henrich et al., 2005). Therefore, there might be less efficient processing of zebrafish meprin α_2. In contrast, Marchand et al. (1995) showed that mutations

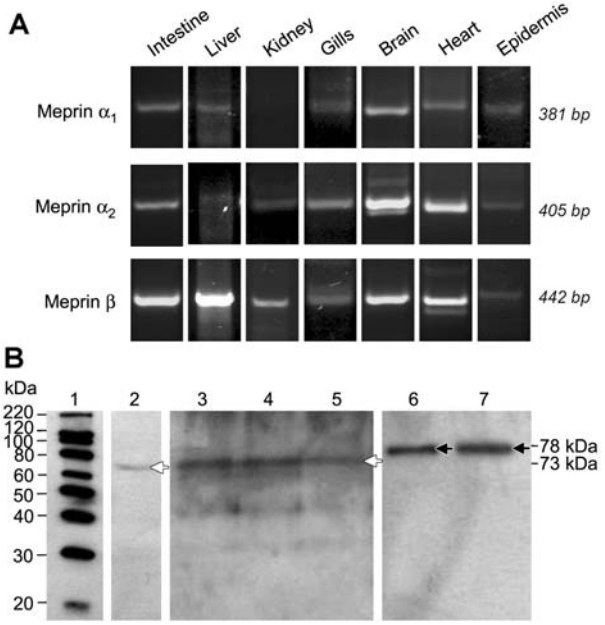

Figure 5 Detection of meprins in different zebrafish tissues via RT-PCR and Western blot analysis.
(A) All three subunits, two α and one β, were identified at the mRNA level in several tissues, except for α_1 in kidney. The gene-specific primers used flank PCR fragments of 381 bp (meprin α_1), 405 bp (meprin α_2) and 442 bp (meprin β). (B) At the protein level, meprins could be detected using antibodies directed against the homologous human proteins. Samples of whole fish lysates were subjected to SDS-gelectrophoresis and immunoblotting. The bands detected (white arrows) most likely pinpoint the active protease with a molecular mass of approximately 73 kDa (lanes 2–5). As controls, recombinant human meprin zymogens (78 kDa) were loaded (black arrows; meprin α, lane 6; meprin β, lane 7).

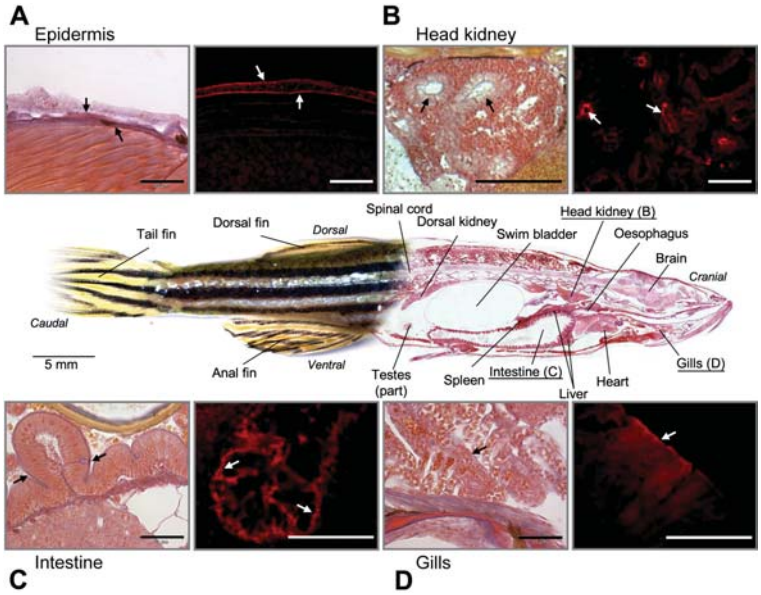

Figure 6 Tissue distribution of zebrafish meprins in whole-mount sections.
The small images show a magnification of meprin-expressing tissues on the left and the expression pattern visualised by immunofluorescence microscopy on the right. In general, in mammals and in zebrafish, meprin expression occurs in the same tissues, such as kidney (head kidney, B) and intestine (C). In addition, in *Danio rerio* fluorescence signals could be detected in the epidermis (A) and gills (D). The white arrows indicate the fluorescence signals based on meprin expression, while the black arrows mark the orientation of these signals inside the corresponding tissue (scale bars represent 50 μm).

in the furin cleavage site did not prevent C-terminal proteolytic processing, whereas deletion of the I-domain resulted in accumulation of unprocessed subunits (Marchand et al., 1994, 1995). It might be assumed that zebrafish α_2 and *Xenopus* meprin α subunits, which lack the complete I-domain, are not C-terminally cleaved during biosynthesis. However, it is remarkable that these subunits still contain the conserved furin-like cleavage site. Zebrafish meprin α_1 lacks the complete C-terminal part, including the EGF, transmembrane and cytosolic domains, due to a stop codon at the beginning of the region encoding the I-domain. Therefore, no posttranslational processing is necessary to obtain soluble protein. In this context, mutagenesis studies of the I-domains of mouse meprin α showed that the enzyme, truncated after the TRAF domain, is secreted directly after biosynthesis (Marchand et al., 1994). A recent database entry [Swiss-Prot accession no. Q08CC4], identical to Q5RH57, shows an elongated C-terminal sequence for the β subunit. It contains the transmembrane and cytosolic domains, but not the EGF-like domain. This striking difference in amino acid sequence in comparison to mammalian homologues could also be identified by *in silico* analysis of the genomic DNA (data not shown).

Table 1 Comparison of meprin-expressing tissues from zebrafish and mammals.

Tissue	Human	Mouse	Zebrafish	
			mRNA	Protein
Intestine	+	+	+	+
Kidney	+	+	+	+
Liver and pancreas	?	+	+	?
Respiratory organs	?	?	+	+
Epidermis	+	+	+	+
Brain	+	+	+	?
Leukocytes, tumour cells	+	+	?	?

+, meprin expression sites already identified; ?, tissues for which meprin expression has not been reported so far.

The phylogenetic tree reveals the evolutionary relationship between zebrafish and mammalian meprins. It is evident that the meprin β cluster arose before the α subunits, which means that the membrane-bound form of the protease is the precursor molecule. The α subunits originated presumably by duplication of the β gene. At a later stage, insertion of the I-domain into the α gene gave rise to a new secreted enzyme, for which the C-terminal part, including the membrane anchor, is cleaved off in the secretory pathway. This leads to evolution of protease activity at a completely new destination, apart from cell surface proteins.

Human, mouse and rat meprin subunits can cleave a wide variety of substrates *in vitro*. Based on sequence alignments and computer modelling of the zebrafish subunits, essential differences in cleavage specificity of both subunits can be expected in comparison to mammalian meprins. For example, human and mouse meprin β contain positively charged residues, namely Arg147 and Lys185 in mouse and Arg85 and Arg123 in human in the S1′ and S2′ positions. These amino acids are responsible for the preference of acidic side chains in P1′ and P2′ substrate positions (Villa et al., 2003; Kruse et al., 2004). Human and mouse meprin α does not contain charged residues in the corresponding positions, leading to broader subsite specificity (Kruse et al., 2004). Tyr122 in human meprin α has been suggested to serve as a 'gatekeeper', which controls entrance into the active site cleft. The importance of these positions has been dem-

onstrated by site-directed mutagenesis in mouse meprin α, which was able to cleave gastrin, a meprin β specific substrate, after exchange of a hydrophobic (Tyr199) to a basic amino acid (Lys199) (Villa et al., 2003). In contrast to all mammalian meprins, the β subunit of *D. rerio* contains just one positively charged residue (Lys123) in the presumed S1′ subsite. In contrast, both meprin α_1 and α_2 contain charged residues in positions critical for substrate binding. These are Asp61 and Arg150, as well as Glu80 and Lys122 in α_2; the latter is also present in the β subunit. With regard to human and mouse meprins, these molecular differences most likely affect the cleavage specificity of zebrafish meprins and presumably also their physiological functions.

The distribution of zebrafish meprins *in situ* has been demonstrated by immunofluorescence microscopy using primary antibodies directed against epitopes of human meprins. Unfortunately, the antisera do not allow discrimination between the α and β subunits, or between the inactive pro form and the active form in zebrafish. Nevertheless, the expression pattern in intestine, epidermis and kidney is obviously comparable to that of mammals. Moreover, zebrafish liver and head kidney also exhibit strong meprin expression. The phylogenetically old head kidney mainly acts as a haematopoietic and lymphoid organ, producing lymphocytes and erythrocytes (Rijkers, 1981; Willett et al., 1999; Trede et al., 2004). These findings support a possible immunological role of meprins. This potential function was originally suggested owing to meprin expression in mammalian leukocytes of the intestinal lamina propria mucosae and in macrophages of mesenterial lymph nodes (Lottaz et al., 1999a). Furthermore, meprin β knockout mice show an immune-deficient phenotype (Crisman et al., 2004). Functional evidence of an immunological role of meprins has been provided by the observation that meprin β can activate interleukin-1β, which facilitates the differentiation of B- and T-cells (Crisman et al., 2004; Herzog et al., 2005).

At the mRNA level, the well-described expression loci for meprin in mammals, the intestine and kidney, could be verified for zebrafish. In addition, meprin expression has been shown in zebrafish heart and brain. The presence of meprin mRNA could also be identified in mouse brain (data not shown) and in brain ventricles and the choroid plexus during rat embryonic development by *in situ* hybridisation experiments (Spencer-Dene et al., 1994; Becker-Pauly et al., 2007).

In zebrafish we also found that the respiratory organs were positive for meprin expression, where the enzymes were identified in epithelial cells of the gill lamellae at the mRNA and protein levels. Interestingly, meprins are also present in zebrafish epidermis. This correlates well with the observation of meprin subunits in human keratinocytes (Becker-Pauly et al., 2007), where both subunits are not colocalised, but expressed in epidermal cells of the basal layer (meprin α) and in more differentiated keratinocytes of the stratum granulosum (meprin β). These expression loci indicate possible functions of these proteases during cell proliferation (meprin α) and differentiation (meprin β) with regard to the influence of human meprins on cultured HaCaT cells. Similar observations have been made in mice suffering acute renal dysfunction (Carmago et al., 2002).

Conclusions

We have shown that the expression of meprin metalloproteinases is not restricted to mammals or to the limited number of tissues reported previously. The cDNA and amino acid sequences of zebrafish meprins are indicative of many similarities with their mammalian counterparts. However, there are also many individual properties that should affect secretion and cleavage specificity. Taken together, these observations open a new research field to study the physiological functions of meprins in a well-described animal model.

Materials and methods

All chemicals were of analytical grade and, unless stated otherwise, were obtained from Amersham Bioscience (Freiburg, Germany), Applichem (Darmstadt, Germany), Serva (Heidelberg, Germany), Bio-Rad (Munich, Germany), Bachem (Heidelberg, Germany), Sigma/Aldrich (Deisenhofen, Germany) or Merck (Darmstadt, Germany). For all experiments, ultrapure water generated by a Milli-Q system (Millipore, Eschborn, Germany) was used.

Fish maintenance

Zebrafish (*Danio rerio*) were bred and kept under constant conditions at a temperature of 28°C and a schedule of 14 h of light and 10 h of darkness. From embryonic stadium, fish were fed daily with dry food and monthly with living food (*Artemia salina*).

RNA isolation and reverse transcription PCR

All materials for RNA isolation and PCR were obtained from Peqlab (Erlangen, Germany). Water containing diethylpyrocarbonate (DEPC) as an inhibitor for RNases was used for all work on RNA and DNA.

Total RNA from zebrafish was prepared from tissues using the peqGOLD Total RNA Kit. Equal amounts of RNA (1 μg) were transcribed into cDNA in 25-μl reaction mixtures using MMLV-Reverse Transcriptase (200 U/μl), unspecific oligo $d(T)_{18-21}$ primers (10 mM; Roth, Karlsruhe, Germany), additional RNase inhibitor (30 U/μl) and dNTPs (200 μM). After transcription, 2 μl of the newly synthesised cDNA was used as a template for PCR, which was performed with 2.5 U of Taq DNA polymerase (GoTaq; Promega, Mannheim, Germany), 200 μM dNTP Mix and 0.2 pM of each primer (sense and antisense).

The following primers (Biomers, Ulm, Germany) were used: meprin α_1 (Swiss-Prot accession no. Q5RHM1), sense 5′-CGGCTGTGATCATAAGGCTGT-3′, antisense 5′-CAAAAGCACACTGGTCCAGC-3′; meprin α_2 (Q5RHM2), sense 5′-TCCCAAAGAGAATTGTTTGAA-3′, antisense 5′-AATGATTTGATCCCACCAGAT-3′; and meprin β (Q5RH57), sense 5′-TGCATTGACTTTAAACCTTGG-3′, antisense 5′-TCAGCTTGAGCAAATCATTGT-3′. After initial denaturation at 95°C for 5 min, PCR was carried out for 45 cycles of 94°C for 60 s, 56°C for 30 s and 72°C for 60 s. Equal amounts of the PCR products were visualised by separation on a 1% agarose gel containing 0.04% ethidium bromide.

Sequencing of purified PCR fragments was performed by GENterprise (Mainz, Germany).

Cell lysis and Western blot analysis

Homogenised fish were incubated in lysis buffer (137 mM NaCl, 2.7 mM KCl, 9.2 mM Na_2HPO_4, 1.8 mM KH_2PO_4, 1% Triton X-

100, pH 7.4) overnight at 4°C. After separation from cell debris by centrifugation at 13 200 *g* for 5 min, the lysate was concentrated using Amicon centrifugal filter units with an exclusion size of 50 kDa (Millipore).

For immunoblot analysis, proteins were subjected to 10% SDS-PAGE (Laemmli, 1970) under reducing conditions and then transferred to a polyvinylidene fluoride (PVDF)-membrane (Immobilon P, Millipore) by electroblotting (80 mA, 75 min). For detection with meprin-specific antibodies, the membrane was saturated with 5% dry milk in Tris-buffered saline (TBS) for 1 h at room temperature, incubated with the first antibody (polyclonal rabbit anti-meprin antibodies, 1:1000) for 1 h and then with horseradish peroxidase-conjugated anti-rabbit IgG (1:10 000) for 45 min at room temperature. Detection was performed with Rotilumin (Roth) according to the manufacturer's instructions using X-ray film (Hyperfilm ECL, Amersham Pharmacia Biotech, Freiburg, Germany). Magic Mark XP (Invitrogen, Karlsruhe, Germany) was used as a molecular mass marker.

Alignments and homology models

The catalytic domains of zebrafish meprins were aligned against one another and mammalian meprin catalytic domains using the ClustalX method (Thompson et al., 1997). They were edited using GeneDoc software (Nicholas et al., 1997).

After alignment, the molecular structures of the catalytic domains were predicted using the SwissMODEL module (Kopp and Schwede, 2004). Modelling was performed with the SwissPDB Viewer software (Kaplan and Littlejohn, 2001) based on the crystal structure of astacin from *Astacus astacus* (Bode et al., 1992).

Phylogenetic trees of meprins from different species were computed with MrBayes software (Ronquist and Huelsenbeck, 2003) using the PAM-Dayhoff distance matrix and consensus trees were visualised using TreeView software (Page, 1996).

Whole-mount tissue fixation, embedding and cutting of zebrafish

For an anatomical overview, adult zebrafish were fixed in Bouin's fixative [150 ml of ethanol, 1 g of picric acid, 60 ml of formaldehyde (37%), 15 ml of acetic acid] for 48 h (Ortiz-Hidalgo, 1992). After washing in an ethanol series (from 70% to 96% in four steps), the fixed zebrafish were embedded in methacrylate, dried for 48 h at 50°C and 60°C, and finally stained with Cason's Trichrom stain (Cason, 1950). Collagen-rich and reticular tissues and acid mucosubstances are coloured in blue, while erythrocytes, glia fibrils and nuclei are stained in red. After staining, sections of 10 μm in thickness were cut on a SuperCut microtome (Leica Microsystems, Wetzlar, Germany). The samples were viewed and visualised using a Zeiss Axioskop microscope (Zeiss, Jena, Germany) with bright-field and differential interference contrast (DIC) optics.

Immunofluorescence analysis

Cryosections of unfixed adult zebrafish prepared with a HM 560 cryostat (Microm, Walldorf, Germany) were incubated with 5% goat serum in phosphate-buffered saline (PBS; 137 mM NaCl, 2.7 mM KCl, 9.2 mM Na_2HPO_4, 1.8 mM KH_2PO_4, pH 7.4) to block non-specific binding. Then the samples were incubated for 2 h at 4°C with polyclonal serum antibodies (1:200 in 0.5% goat serum/PBS). Cross-reactive rabbit polyclonal antisera were generated against two peptides. One is directed against a fragment of 420 aa including the propeptide, the protease and MAM domain of human meprin α. The other recognises a peptide comprising 150 aa of the TRAF domain of the human β subunit. All antigen peptides were expressed in *Escherichia coli* (Dumermuth et al., 1993; Lottaz et al., 1999a). After removal of unbound primary antibody by washing with PBS, the samples were incubated with Alexa 568 goat anti-rabbit IgG fluorescent antibody (1:400 in 0.5% goat serum/PBS, Invitrogen) for 90 min. 4,6-Diamidino-2-phenylindol (DAPI) was added to label the nuclei. Immunofluorescence detection was carried out using a Zeiss Axioskop microscope with fluorescence capability.

Acknowledgements

We thank Katja Lotz for her excellent technical assistance in histology. This work was supported by a start-up grant from the Johannes Gutenberg-University of Mainz to C.B-P., Germany and the Swiss National Science Foundation (Grant no. 3100A0-100772 to E.S.).

References

Becker, C., Kruse, M.N., Slotty, K.A., Kohler, D., Harris, J.R., Rösmann, S., Sterchi, E.E., and Stöcker, W. (2003). Differences in the activation mechanism between the α and β subunits of human meprin. Biol. Chem. *384*, 825–831.

Becker-Pauly, C., Höwel, M., Walker, T., Vlad, A., Aufenvenne, K., Oji, V., Lottaz, D., Sterchi, E.E., Debela, M., Magdolen, V., et al. (2007). The α and β subunits of the metalloprotease meprin are expressed in separate layers of human epidermis, revealing different functions in keratinocyte proliferation and differentiation. J. Invest. Dermatol., DOI: 10.1038/sj.jid.5700675.

Bertenshaw, G.P., Turk, B.E., Hubbard, S.J., Matters, G.L., Bylander, J.E., Crisman, J.M., Cantley, L.C., and Bond, J.S. (2001). Marked differences between metalloproteases meprin A and B in substrate and peptide bond specificity. J. Biol. Chem. *276*, 13248–13255.

Bertenshaw, G.P., Norcum, M.T., and Bond, J.S. (2003). Structure of homo- and hetero-oligomeric meprin metalloproteases. Dimers, tetramers, and high molecular mass multimers. J. Biol. Chem. *278*, 2522–2532.

Bode, W., Gomis-Rüth, F.X., Huber, R., Zwilling, R., and Stöcker, W. (1992). Structure of astacin and implications for activation of astacins and zinc-ligation of collagenases. Nature *358*, 164–167.

Bond, J.S. and Beynon, R.J. (1995). The astacin family of metalloendopeptidases. Protein Sci. *4*, 1247–1261.

Bond, J.S., Rojas, K., Overhauser, J., Zoghbi, H.Y., and Jiang, W. (1995). The structural genes, MEP1A and MEP1B, for the α and β subunits of the metalloendopeptidase meprin map to human chromosomes 6p and 18q, respectively. Genomics *25*, 300–303.

Carmago, S., Shah, S.V., and Walker, P.D. (2002). Meprin, a brush-border enzyme, plays an important role in hypoxic/ischemic acute renal tubular injury in rats. Kidney Int. *61*, 959–966.

Cason, J.E. (1950). A rapid one-step Mallory-Heidenhain stain for connective tissue. Stain Technol. *25*, 225–226.

Crisman, J.M., Zhang, B., Norman, L.P., and Bond, J.S. (2004). Deletion of the mouse meprin β metalloprotease gene diminishes the ability of leukocytes to disseminate through extracellular matrix. J. Immunol. *172*, 4510–4519.

Duckert, P., Brunak, S., and Blom, N. (2004). Prediction of proprotein convertase cleavage sites. Protein Eng. Des. Sel. *17*, 107–112.

Dumermuth, E., Eldering, J.A., Grunberg, J., Jiang, W., and Sterchi, E.E. (1993). Cloning of the PABA peptide hydrolase α subunit (PPH α) from human small intestine and its expression in COS-1 cells. FEBS Lett. *335*, 367–375.

Gomis-Rüth, F.X. (2003). Structural aspects of the metzincin clan of metalloendopeptidases. Mol. Biotechnol. *24*, 157–202.

Hahn, D., Pischitzis, A., Roesmann, S., Hansen, M.K., Leuenberger, B., Luginbuehl, U., and Sterchi, E.E. (2003). Phorbol 12-myristate 13-acetate-induced ectodomain shedding and phosphorylation of the human meprin β metalloprotease. J. Biol. Chem. *278*, 42829–42839.

Henrich, S., Lindberg, I., Bode, W., and Than, M.E. (2005). Proprotein convertase models based on the crystal structures of furin and kexin: explanation of their specificity. J. Mol. Biol. *345*, 211–227.

Herzog, C., Kaushal, G.P., and Haun, R.S. (2005). Generation of biologically active interleukin-1β by meprin B. Cytokine *31*, 394–403.

Ishmael, F.T., Shier, V.K., Ishmael, S.S., and Bond, J.S. (2005). Intersubunit and domain interactions of the meprin B metalloproteinase. Disulfide bonds and protein-protein interactions in the MAM and TRAF domains. J. Biol. Chem. *280*, 13895–13901.

Johnson, G.D. and Hersh, L.B. (1994). Expression of meprin subunit precursors. Membrane anchoring through the β subunit and mechanism of zymogen activation. J. Biol. Chem. *269*, 7682–7688.

Kaplan, W. and Littlejohn, T.G. (2001). Swiss-PDB Viewer (Deep View). Brief Bioinform. *2*, 195–197.

Kaushal, G.P., Walker, P.D., and Shah, S.V. (1994). An old enzyme with a new function: purification and characterization of a distinct matrix-degrading metalloproteinase in rat kidney cortex and its identification as meprin. J. Cell Biol. *126*, 1319–1327.

Kopp, J. and Schwede, T. (2004). The SWISS-MODEL repository of annotated three-dimensional protein structure homology models. Nucleic Acids Res. *32*, D230–D234.

Kruse, M.N., Becker, C., Lottaz, D., Köhler, D., Yiallouros, I., Krell, H.W., Sterchi, E.E., and Stöcker, W. (2004). Human meprin α and β homo-oligomers: cleavage of basement membrane proteins and sensitivity to metalloprotease inhibitors. Biochem. J. *378*, 383–389.

Laemmli, U.K. (1970). Cleavage of structural proteins during the assembly of the head of bacteriophage T4. Nature *227*, 680–685.

Leighton, M. and Kadler, K.E. (2003). Paired basic/Furin-like proprotein convertase cleavage of Pro-BMP-1 in the trans-Golgi network. J. Biol. Chem. *278*, 18478–18484.

Lottaz, D., Hahn, D., Muller, S., Muller, C., and Sterchi, E.E. (1999a). Secretion of human meprin from intestinal epithelial cells depends on differential expression of the α and β subunits. Eur. J. Biochem. *259*, 496–504.

Lottaz, D., Maurer, C.A., Hahn, D., Buchler, M.W., and Sterchi, E.E. (1999b). Nonpolarized secretion of human meprin α in colorectal cancer generates an increased proteolytic potential in the stroma. Cancer Res. *59*, 1127–1133.

Marchand, P., Tang, J., and Bond, J.S. (1994). Membrane association and oligomeric organization of the α and β subunits of mouse meprin A. J. Biol. Chem. *269*, 15388–15393.

Marchand, P., Tang, J., Johnson, G.D., and Bond, J.S. (1995). COOH-terminal proteolytic processing of secreted and membrane forms of the α subunit of the metalloprotease meprin A. Requirement of the I domain for processing in the endoplasmic reticulum. J. Biol. Chem. *270*, 5449–5456.

Nicholas, K.B., Nicholas, H.B. Jr., and Deerfield, D.W. (1997). GeneDoc: analysis and visualization of genetic variation. EMBNEW News *4*, 14.

Norman, L.P., Jiang, W., Han, X., Saunders, T.L., and Bond, J.S. (2003). Targeted disruption of the meprin β gene in mice leads to underrepresentation of knockout mice and changes in renal gene expression profiles. Mol. Cell. Biol. *23*, 1221–1230.

Ortiz-Hidalgo, C. (1992). Pol Andre Bouin, MD (1870–1962). Bouin's fixative and other contributions to medicine. Arch. Pathol. Lab. Med. *116*, 882–884.

Page, R.D. (1996). TreeView: an application to display phylogenetic trees on personal computers. Comput. Appl. Biosci. *12*, 357–358.

Rijkers, G.T. (1981). Introduction to fish immunology. Dev. Comp. Immunol. *5*, 527–534.

Ronquist, F. and Huelsenbeck, J.P. (2003). MrBayes 3: Bayesian phylogenetic inference under mixed models. Bioinformatics *19*, 1572–1574.

Rösmann, S., Hahn, D., Lottaz, D., Kruse, M.N., Stöcker, W., and Sterchi, E.E. (2002). Activation of human meprin-α in a cell culture model of colorectal cancer is triggered by the plasminogen-activating system. J. Biol. Chem. *277*, 40650–40658.

Skidgel, R.A. (1992). Bradykinin-degrading enzymes: structure, function, distribution, and potential roles in cardiovascular pharmacology. J. Cardiovasc. Pharmacol. *20* (Suppl. 9), S4–S9.

Spencer-Dene, B., Thorogood, P., Nair, S., Kenny, A.J., Harris, M., and Henderson, B. (1994). Distribution of, and a putative role for, the cell-surface neutral metallo-endopeptidases during mammalian craniofacial development. Development *120*, 3213–3226.

Sterchi, E.E., Green, J.R., and Lentze, M.J. (1982). Non-pancreatic hydrolysis of *N*-benzoyl-L-tyrosyl-*p*-aminobenzoic acid (PABA-peptide) in the human small intestine. Clin. Sci. (Lond.) *62*, 557–560.

Sterchi, E.E., Green, J.R., and Lentze, M.J. (1983). Nonpancreatic hydrolysis of *N*-benzoyl-L-tyrosyl-*p*-aminobenzoic acid (PABA peptide) in the rat small intestine. J. Pediatr. Gastroenterol. Nutr. *2*, 539–547.

Sterchi, E.E., Naim, H.Y., Lentze, M.J., Hauri, H.P., and Fransen, J.A. (1988). *N*-Benzoyl-L-tyrosyl-*p*-aminobenzoic acid hydrolase: a metalloendopeptidase of the human intestinal microvillus membrane which degrades biologically active peptides. Arch. Biochem. Biophys. *265*, 105–118.

Stöcker, W., Gomis-Rüth, F.X., Bode, W., and Zwilling, R. (1993). Implications of the three-dimensional structure of astacin for the structure and function of the astacin family of zinc-endopeptidases. Eur. J. Biochem. *214*, 215–231.

Stöcker, W., Grams, F., Baumann, U., Reinemer, P., Gomis-Rüth, F.X., McKay, D.B., and Bode, W. (1995). The metzincins – topological and sequential relations between the astacins, adamalysins, serralysins, and matrixins (collagenases) define a superfamily of zinc-peptidases. Protein Sci. *4*, 823–840.

Thompson, J.D., Gibson, T.J., Plewniak, F., Jeanmougin, F., and Higgins, D.G. (1997). The CLUSTAL_X windows interface: flexible strategies for multiple sequence alignment aided by quality analysis tools. Nucleic Acids Res. *25*, 4876–4882.

Trachtman, H., Valderrama, E., Dietrich, J.M., and Bond, J.S. (1995). The role of meprin A in the pathogenesis of acute renal failure. Biochem. Biophys. Res. Commun. *208*, 498–505.

Trede, N.S., Langenau, D.M., Traver, D., Look, A.T., and Zon, L.I. (2004). The use of zebrafish to understand immunity. Immunity *20*, 367–379.

Villa, J.P., Bertenshaw, G.P., and Bond, J.S. (2003). Critical amino acids in the active site of meprin metalloproteinases for substrate and peptide bond specificity. J. Biol. Chem. *278*, 42545–42550.

Willett, C.E., Cortes, A., Zuasti, A., and Zapata, A.G. (1999). Early hematopoiesis and developing lymphoid organs in the zebrafish. Dev. Dyn. *214*, 323–336.

Yamaguchi, T., Kido, H., and Katunuma, N. (1992). A membrane-bound metallo-endopeptidase from rat kidney. Characteristics of its hydrolysis of peptide hormones and neuropeptides. Eur. J. Biochem. *204*, 547–552.

Yiallouros, I., Kappelhoff, R., Schilling, O., Wegmann, F., Helms, M.W., Auge, A., Brachtendorf, G., Berkhoff, E.G., Beermann, B., Hinz, H.J., et al. (2002). Activation mechanism of proastacin: role of the pro-peptide, tryptic and autoproteolytic cleavage and importance of precise amino-terminal processing. J. Mol. Biol. *324*, 237–246.

Received January 3, 2007; accepted February 16, 2007